# Structure-Activity Relationship Studies Reveal New Astemizole Analogues Active against *Plasmodium falciparum* In Vitro

Dickson Mambwe,† Malkeet Kumar,†Ω Richard Ferger,† Dale Taylor,‡ Mathew Njoroge,‡ Dina Coertzen⊥, Janette Reader⊥, Mariëtte van der Watt⊥, Lyn-Marie Birkholtz,⊥ and Kelly Chibale†,‡,○,*

*†Department of Chemistry, University of Cape Town, Rondebosch 7701, South Africa.*
*‡Drug Discovery and Development Centre (H3D), Division of Clinical Pharmacology, Department of Medicine, University of Cape Town, Observatory 7925 , South Africa.*
*⊥Department of Biochemistry, Genetics & Microbiology, Institute for Sustainable Malaria Control, University of Pretoria, Private Bag X20, Hatfield 0028, Pretoria, South Africa.*
*○Institute of Infectious Disease and Molecular Medicine, University of Cape Town, Rondebosch 7701, South Africa.*
**South African Medical Research Council Drug Discovery and Development Research Unit, University of Cape Town, Rondebosch 7701, South Africa.*
*ΩCurrent address: Institute of Chemistry, Department of Organic Chemistry, Universidade Estadual de Campinas, Campinas, São Paulo 13083-970, Brazil.*

*Corresponding Author:
Kelly Chibale − Department of Chemistry, Institute of Infectious Disease and Molecular Medicine, and South African Medical Research Council Drug Discovery and Development Research Unit, University of Cape Town, Rondebosch 7701, South Africa; Drug Discovery and Development Centre (H3D), Division of Clinical Pharmacology, Department of Medicine, University of Cape
Town, Observatory 7925, South Africa; Email: kelly.chibale@uct.ac.za

## Graphical abstract

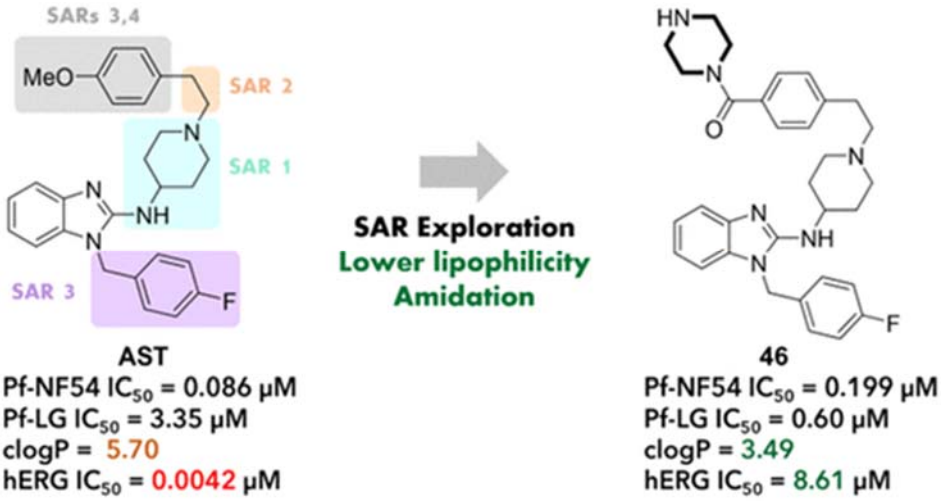

## Abstract

In the context of drug repositioning and expanding the existing structure-activity relationship around astemizole (AST), a new series of analogues were designed, synthesized, and evaluated for their antiplasmodium activity. Among 46 analogues tested, compounds **21**, **30**, and **33** displayed high activities against asexual blood stage parasites (*Pf*NF54 $IC_{50}$ = 0.025-0.043 μM), whereas amide compound **46** additionally showed activity against late-stage gametocytes (stage IV/V; *Pf*LG $IC_{50}$ = 0.6 ± 0.1 μM) and 860-fold higher selectivity over hERG (**46**, SI = 43) compared to AST. Several analogues displaying high solubility (Sol > 100 μM) and low cytoxicity in the Chinese hamster ovary (SI > 148) cell line have also been identified.

**KEYWORDS:** Astemizole; *Plasmodium falciparum*; repositioning; human ether-a-go-go-related gene

Malaria is a life-threatening disease caused by *Plasmodium* parasites transmitted to humans via *Plasmodium*-infected *Anopheles* mosquitoes during a blood meal. Among the five human malaria species known, *P. falciparum* (*Pf*) is the most virulent and highly prevalent in the African region. [1−3] According to the 2020 WHO World Malaria Report, an estimated 229 million cases of malaria were recorded worldwide in 2019, with the sub-Saharan African region bearing the largest burden, accounting for 94% of the global incidence rate. [3] During that year, 409,000 deaths occurred, among which 67% were children under the age of 5, [3] maintaining the death rate of "one-child every 2 min" statistic.

The use of antimalarial drugs forms the cornerstone of both the prevention and treatment of the disease. Currently, the WHO recommends the use of the artemisinin-based combination therapy (ACT) regimen, which has provided both treatment and protection to millions over the last few decades. [4,5] However, the continuous evidence of the emergence of resistance in countries of the Greater Mekong Subregion (GMS) and more recently in the African Great Lakes region, particularly Rwanda, poses a serious threat to the current regimen. [6,7] Therefore, the need to utilize various approaches to discover and develop new and structurally diverse antimalarials that offer both chemoprotection and prevent reinfection via multistage activity is warranted.

Chong and co-workers identified the antimalarial properties of the antihistamine drug astemizole (AST) and its principal metabolite desmethylastemizole (DM-AST) via a high-throughput screen (HTS) of 2687 existing drugs. Both AST and DM-AST showed growth inhibition of chloroquine-sensitive (CQ-S) and multi-drug-resistant (MDR) malaria parasites, which translated to parasitemia reduction in two in vivo mouse models of malaria. Furthermore, preliminary mode of action studies revealed that AST exhibits its antimalarial action by accumulating in the *Pf* food vacuole, thereby disrupting heme crystallization. [8] However, the presence of additional mechanism(s) was not ruled out. AST has also previously been shown to possess liver-stage antimalarial activity ($IC_{50}$ = 0.114 μM) from a HTS screen of 5375 known drugs with diverse modes of actions using *P. berghei* (*Pb*) parasites. [9]

Notably, various researchers have used AST as a template to derive analogues with varying degrees of antiplasmodium activity. Musonda and co-workers explored the potential to

overcome *Pf* resistance to chloroquine (CQ) via hybridization with the AST pharmacophore. Front-runner compounds from this work demonstrated improved in vitro activity against the K1 CQ-R strain of *Pf* ($IC_{50}$ = 0.037–0.610 μM) as well as high in vivo efficacy in the *Pb* mouse infection model of malaria. [10] Additionally, two recent publications separately conducted brief antiplasmodium structure–activity relationship (SAR) studies based on AST. [11,12] The summary of SAR studies reported by De Jonghe and co-workers showed that the most potent analogues from their series also demonstrated reduced hERG channel inhibition activity (SI = 110). [12] However, the cytotoxicity of these analogues was not reported, and the poor drug likeness evidenced by high lipophilicity (clog*P* = 7.7) and low solubility of the front-runner compound would present challenges in development.

Our group previously showed the potential of AST and its analogues to display multistage activity against *Plasmodium* parasites following their evaluation against asexual blood stage (*Pf*NF54 $IC_{50}$ = 0.033–1.9 μM), liver stage (*Pb* $IC_{50}$ = 0.210 μM), and late-stage gametocytes (stage IV/V; *Pf*LG $IC_{50}$ = 1.9–4.1 μM). Additionally, we showed intracellular inhibition of hemozoin formation by AST analogues within the parasite, which supported Chong and co-workers' initial findings of AST's interference with the heme detoxification pathway. [13] These results justified further investigation of the AST scaffold toward its optimization for malaria. In the present work, several structural analogues of AST were designed with the goal of improving antiplasmodium activity and enhancing solubility while utilizing known strategies to circumvent the human ether-a-go-go-related gene (hERG) potassium ($K^+$) channel inhibition liability associated with AST.

The SAR buildup involved modifications of various parts of AST categorized in four regions (Figure 1). Among the strategies to reduce hERG affinity and improve aqueous solubility, we utilized reducing lipophilicity (clog*P*), removal of aromaticity, attenuating the p$K_a$ of the basic nitrogen, as well as discrete modifications around the AST scaffold.

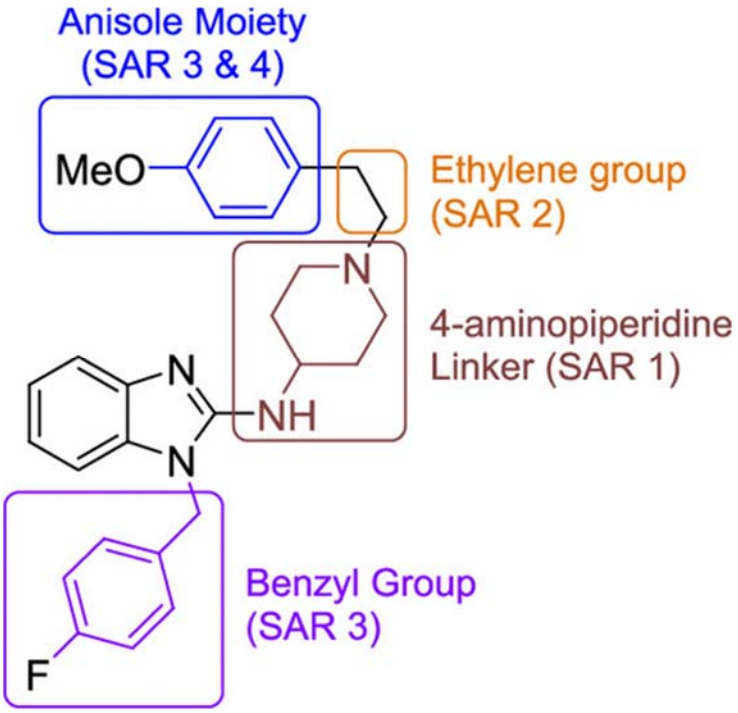


**Figure 1**. Summary of designed SAR around AST.

SAR 1 involved the replacement of the 4-aminopiperidine linker with open chain diamine alkyl moieties (Figure 1), whereas SAR 2 was designed to reduce the p$K_a$ of the basic piperidine nitrogen via incorporation of a carbonyl (C═O) group at the α- and β-position on the ethylene group. SAR 3 was focused on replacing the 4-OMe and 4-F groups of the anisole and benzyl groups, respectively, with representative substituents from each of the four quadrants of the Craig plot. In the benzyl moiety, truncation, replacement with methyl, incorporation of heteroatom (N), methylation of the methylene bridge, and CN/F disubstitution were also explored in SAR 3. Toward reducing hERG affinity, replacement of the 4-OMe group in the anisole moiety with amides was explored in SAR 4 (Figure 1). Similarly, the anisole group was replaced with both aliphatic and aromatic heterocycles (SAR 4) to expand the SAR and interrogate the significance of the phenyl group.

The synthesis of SAR 1 and 2 analogues commenced with the coupling of commercially available 2-chloro-1-(4-fluorobenzyl)-1*H*-benzo[*d*]imidazole (Scheme 1) with various diamines, resulting in intermediates **1a**–**c** and **5**. In SAR 1, nucleophilic substitution reactions between amines **1a**–**c** and 4-methoxyphenethyl bromide in the presence of triethylamine ($NEt_3$) in *N*,*N*-dimethylformamide (DMF) afforded target compounds **2**–**4**. For SAR 2, deprotection of **5** followed by coupling of the resulting free amine (**6**) to commercially sourced 2-bromo-1-(4-methoxyphenyl)ethan-1-one and 2-(4-methoxyphenyl)acetic acid resulted in compounds **7** and **8**, respectively. [13]

**Scheme 1.**

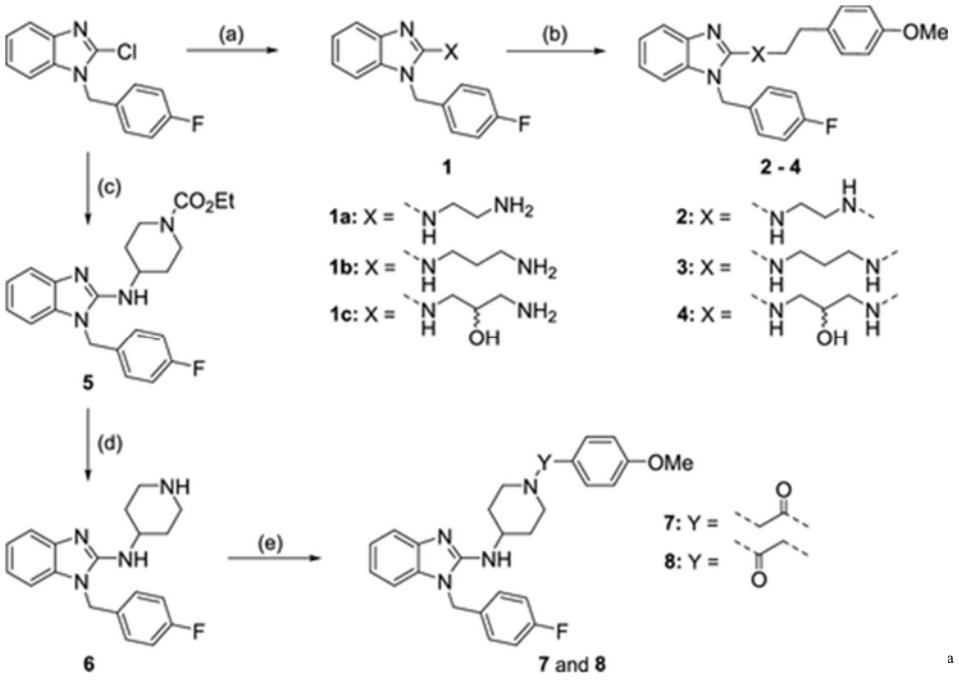


[a]Reagents and conditions: (a) ethane-1,2-diamine (for **1a**) or propane-1,3-diamine (for **1b**), 120 °C, 8–12 h (**1a**; 85%, and **1b**; 92%); 1,3-diaminopropan-2-ol, EtOH, 79 °C, 96 h (**1c**; 50%); (b) 4-methoxyphenethyl bromide, $Et_3N$, DMF, 22 °C, 10 h (15–62%); (c) ethyl 4-aminopiperidine-1-carboxylate, 170 °C, 4 h (98%); (d) 48% aq HBr, 120 °C, 3 h (85%); (e) 2-bromo-1-(4-methoxyphenyl)ethan-1-one, $Et_3N$, DCM, 22 °C (**7**; 10%); 2-(4-methoxyphenyl)acetic acid, $T_3P$, *i*-$Pr_2NEt$, DMF, 0–22 °C, 3 h (**8**; 55%).

Compounds containing modifications in the benzyl group (**12**–**26**, SAR 3) and the anisole moiety (**27**–**53**, SAR 4) were synthesized, as shown in Scheme 2. The synthesis of respective

alkylating agents (**9a**–**g**) required to deliver target compounds in Scheme 2 is described in Supporting Information (Scheme S1).

**Scheme 2.**

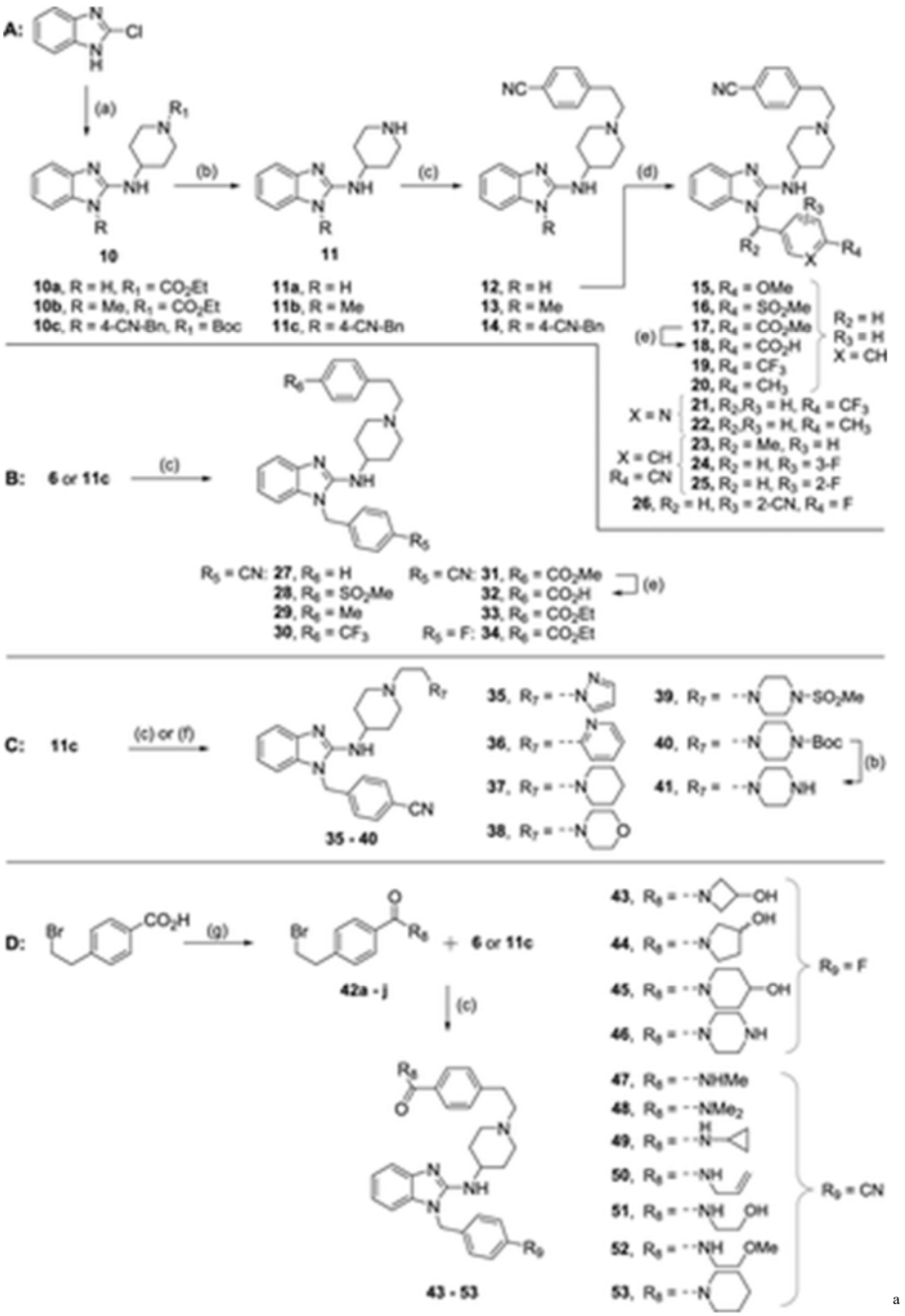

[a]Reagents and conditions: (a) (i) alkylating agent, $K_2CO_3$, acetone, 18–23 °C, 2–5 h (60–98%); (ii) ethyl 4-aminopiperidine-1-carboxylate or *tert*-butyl 4-aminopiperidine-1-carboxylate, $Et_3N$, 150 °C, 2–12 h (58–89%); (b) 48% aq HBr, 120 °C, 3 h or TFA, DCM, 20 °C, 3 h, Amberlyst-A21, DCM, 3 h (58–98%); (c) **9a** (for **12**–**14**), or alkylating agent (for **27**–**30**) or **9c** (for **31**) or **9d** (for **33** and **34**), $K_2CO_3$, MeCN, 80–85 °C (32–89%); (d) **9f** (for **23**) or respective alkylating agent, $K_2CO_3$, DMF, 70 °C (73–93%); (e) (i) 2 M KOH, MeOH, 80 °C, 4 h; (ii) 2 N HCl, 0–4 °C, pH 2 (90–96%); (f) 2-(piperazinyl)ethanol (for **39**) and **9g** (for **40**), MsCl, $Et_3N$, DCM, 0–45 °C, 4 h (**39**: 65%; **40**: 46%); (g) amine, *i*-$Pr_2NEt$, $T_3P$, DCM, 23°C, 4–24 h (15–74%).

Briefly, alkylation of 2-chloro-1*H*-benzo[*d*]imidazole at N-1, followed by coupling with ethyl 4-aminopiperidine-1-carboxylate or *tert*-butyl 4-aminopiperidine-1-carboxylate furnished intermediates **10a**–**c**. Following acidic deprotection, free amines (**11a**–**c**) were coupled with 4-(2-bromoethyl)benzonitrile (**9a**, Scheme S1) to afford **12**–**14** in good yields. [13] Treatment of **12** with various benzyl bromides or bromomethylpyridines afforded the target compounds **15**–**17** and **19**–**26** (Scheme 2A), [11] whereas intermediates **27**–**31** and **33**–**40** (Scheme 2C) were accessed using **6** or **11c** via nucleophilic substitution ($S_N2$) with various commercially available or previously synthesized alkylating agents (**9c**,**d** and **9f**,**g**, Scheme S1). Carboxylic acid derivatives **18** and **32** were prepared via hydrolysis of methyl esters **17** and **31**, respectively, whereas piperazine compound **41** was obtained from **40** by TFA N-Boc deprotection (Scheme 2A–C).

Compounds **43**–**53** were obtained via $S_N2$ coupling of either **6** or **11c** with amide derivatives (**42a**–**j**) of 4-(2-bromoethyl)benzoic acid prepared using propanephosphonic acid anhydride ($T_3P$)-mediated acid–amine coupling (Scheme 2D).

All synthesized compounds were evaluated for their solubility and antiplasmodium activity against the chloroquine-sensitive (NF54) strain of *Pf*. Furthermore, selected compounds with $IC_{50}$ < 0.700 μM against *Pf*NF54 were evaluated against the *Pf*K1 (MDR) strain to assess potential for cross-resistance with known antimalarials (i.e., CQ). We previously reported AST analogues exhibiting signatures attributable to possible interaction with the parasitic heme detoxification machinery; (13) for this reason, a representative set of analogues from this series were also assessed for their ability to block β-hematin (β-H) formation, as a surrogate for the inhibition of heme detoxification by the parasite.

Potency was reduced by 4–8-fold when the 4-aminopiperidine group in AST was replaced with an open chain diamine (compounds **2**–**4**; Table 1) in SAR 1.

We next investigated the effect of reducing the basicity of piperidine nitrogen. Activity was lost in both β-keto and amide analogues **7** (*Pf*NF54 $IC_{50}$ = 3.18 μM, Table 1) and **8** (*Pf*NF54 $IC_{50}$ = 2.89 μM) compared to AST. This observation was consistent with previously reported results by De Jonghe and co-workers, which showed loss of activity in urea and sulfonamide analogues. [12] This may suggest the significance of piperidine nitrogen basicity toward antiplasmodium activity. Solubility was generally high in all open chain amine-containing analogues (**2**–**4**) and acylated compound **7** (Sol > 190 μM). However, amide derivative **8** displayed significantly lower solubility (Sol = 60 μM) albeit higher than that of AST. All analogues in this SAR exhibited low βH inhibition ($IC_{50}$ > 1000 μM) with the exception of hydroxy compound **4** ($IC_{50}$ = 94.6 μM, Table S1, Supporting Information).

**Table 1.** In Vitro Antiplasmodium Activity and Solubility of AST Analogues in SARs 1 and 2 (ND, Not Determined)

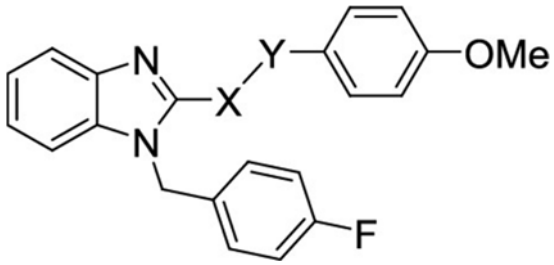


| Compound | X | Y | *Pf* $IC_{50}$ (μM)[a,b] NF54 | *Pf* $IC_{50}$ (μM)[a,b] K1 | RI[c] | Sol.[d] (μM) |
|---|---|---|---|---|---|---|
| AST | 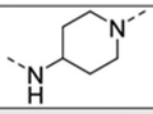 | | 0.086 | 0.370 | 4.30 | 40 |
| **2** | 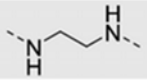 |  | 0.691 | 0.787 | 1.14 | 190 |
| **3** |  | | 0.330 | 0.677 | 2.05 | 200 |
| **4** | 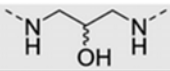 | | 0.706 | 1.406 | 3.46 | 200 |
| **7** | 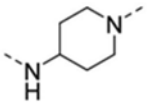 |  | 3.180 | ND | - | 200 |
| **8** | | 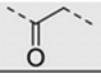 | 2.890 | ND | - | 60 |

[a]Mean from $n \geq 2$ independent experiments with sensitive (NF54) and multi-drug-resistant (K1) strains of *Pf*. [b]Chloroquine (NF54 $IC_{50}$ = 0.004 μM; K1 $IC_{50}$ = 0.14 μM) was used as a reference drug for activity. [c]Resistance index = [*Pf*K1 $IC_{50}$/*Pf*NF54 $IC_{50}$]. [d]Solubility, determined using turbidimetric method at pH 7.4. Hydrocortisone (>200 μM) and reserpine (<10 μM) were used as control drugs.

For the exploration of the benzyl group SAR (SAR 3), the 4-aminopiperidine was retained due to its significance toward potency. However, the 4-OMe group in the anisole moiety was replaced with the 4-CN group (Table 2). This switch was driven by the lipophilicity-lowering effects and resilience toward metabolism associated with the cyano group compared to methoxy. [14,15] There was a general loss in antiplasmodium potency across the SAR, with only three analogues (**24**: *Pf*NF54 $IC_{50}$ = 0.071 μM; **21**: *Pf*NF54 $IC_{50}$ = 0.025 μM; and **25**, *Pf*NF54 $IC_{50}$ = 0.108 μM) out of 15, showing activity higher or comparable to that of AST. Removal of the benzyl group resulted in ∼7-fold loss of activity (**12**: *Pf*NF54 $IC_{50}$ = 0.579 μM) compared to that of AST, whereas replacement with a methyl group significantly diminished the activity (**13**: *Pf*NF54 $IC_{50}$ = 5.08 μM). The weak activity of **12** was found to contradict that of a previously reported debenzylated analogue (compound **5c**: $IC_{50}$ = 0.047 μM, Kumar and co-workers) [13] in which removal of the benzyl group with retention of the 4-OMe group in the anisole moiety increased the potency by 2-fold when compared to AST. This observation may, however, suggest the possibility to significantly optimize antiplasmodium potency in debenzylated analogues by exploring substitutions for the 4-OMe group in the anisole moiety.

**Table 2.** In Vitro Antiplasmodium and Solubility of AST Analogues in SAR 3 (ND, Not Determined)

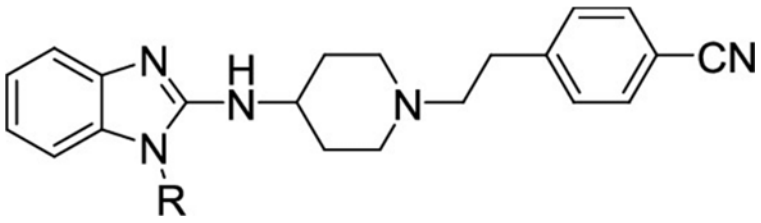

| Compound | R | $R_1$ | *Pf* $IC_{50}$ (μM)[a,b] NF54 | *Pf* $IC_{50}$ (μM)[a,b] K1 | RI[c] | Sol[d] (μM) |
|---|---|---|---|---|---|---|
| **12** | H | - | 0.579 | ND | - | 120 |
| **13** | Me | - | 5.080 | ND | - | 100 |
| **14** |  | CN | 0.156 | 0.176 | 1.1 | 90 |
| **15** | | OMe | 0.624 | ND | - | 50 |
| **16** | | $SO_2Me$ | 0.485 | ND | - | 40 |
| **17** | | $CO_2Me$ | 0.591 | ND | - | 120 |
| **18** | | $CO_2H$ | >6 | ND | - | >200 |
| **19** | | $CF_3$ | 0.253 | 0.384 | 1.5 | 20 |
| **20** | | $CH_3$ | 0.565 | ND | - | 80 |
| **21** | 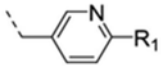 | $CF_3$ | 0.025 | 0.082 | 3.3 | 20 |
| **22** | | $CH_3$ | 0.261 | ND | - | 50 |
| **23** | 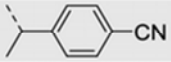 | - | 0.156 | 0.157 | 1.0 | 120 |
| **24** | 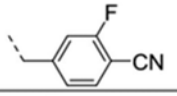 | | 0.071 | 0.211 | 2.9 | 40 |
| **25** | 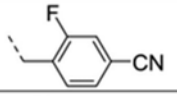 | | 0.108 | ND | - | 20 |
| **26** | 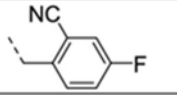 | | 0.185 | 4.013 | 21.7 | 50 |

[a]Mean from $n \geq 2$ independent experiments with sensitive (NF54) and multi-drug-resistant (K1) strains of *Pf*. [b]Chloroquine (NF54 $IC_{50}$ = 0.004 μM; K1 $IC_{50}$ = 0.14 μM) was used as a reference drug for activity. [c]Resistance index = [*Pf*K1 $IC_{50}$/*Pf*NF54 $IC_{50}$]. [d]Solubility, determined using turbidimetric method at pH 7.4. Hydrocortisone (>200 μM) and reserpine (<10 μM) were used as control drugs.

CN/F disubstitution in the benzyl group was generally tolerated, although potency was lowered by ∼2-fold when the CN group was in the *ortho*-position (**26**, *Pf*NF54 $IC_{50}$ = 0.185 μM) compared to that of *ortho*-fluorine (**25**, *Pf*NF54 $IC_{50}$ = 0.108 μM). However, CN/F disubstitution preferentially favored *para*-CN and *meta*-F regioisomerism (**24**, *Pf*NF54 $IC_{50}$ = 0.071 μM, Table 2). Craig plot substitution tends to generally favor electron-withdrawing groups (EWGs) for antiplasmodium potency. However, among the groups tested, only the hydrophilic CN (**14**; *Pf*NF54 $IC_{50}$ < 0.156 μM) and hydrophobic $CF_3$ (**19**; *Pf*NF54 $IC_{50}$ < 0.253 μM) groups are tolerated. Pyridyl analogues **21** and **22** were more potent than their corresponding phenyl (**19** and **20**) match pairs, with the 4-trifluoromethyl-3-pyridyl analogue

(**21**, *Pf*NF54 $IC_{50}$ = 0.025 μM) showing the highest potency in the series (Table 2). With the exception of **26** (*Pf*K1 $IC_{50}$ = 4.0 μM, RI = 21.7), *Pf*K1 data suggested the absence of cross-resistance with existing antimalarial drugs reflected in the low resistance indices (SI < 5).

Consistently, analogues bearing water-solubilizing groups in SAR 3 (**17** and **18**) or devoid of the benzyl aromatic ring (**12** and **13**) exhibited moderate to high solubility (100–200 μM) compared to those containing lipophilic groups such as the F group (**19**, **21**, and **24**–**26**; Sol < 100 μM). Methylation of the benzyl methylene linker was designed to discourage aromatic π–π interactions as a strategy to improve solubility. This effect was indeed observed as the solubility of **23** (Sol = 120 μM) increased compared to that with **14** (Sol = 90 μM) with retention of potency (*Pf*NF54 $IC_{50}$ = 0.156 μM). Three out of eight tested compounds (**14**, **19**, and **25**) displayed β-H inhibition activities of $IC_{50}$ < 100 μM (Table S1).

We next explored various substitutions for the 4-OMe group in the anisole moiety (Table 3). Similar to benzyl group SAR (SAR 3), antiplasmodium activity is generally favored by substitution with EWGs. This is exemplified by the enhanced potency of $CF_3$-substituted **30** (*Pf*NF54 $IC_{50}$ = 0.035 μM). Notably, some EWGs produce activities superior to those of others. For instance, ester analogues **33** (*Pf*NF54 $IC_{50}$ = 0.043 μM) and **34** (*Pf*NF54 $IC_{50}$ = 0.067 μM) showed higher activity than did the methyl ester analogue **31** (*Pf*NF54 $IC_{50}$ = 0.204 μM). On the other hand, activity is lost in the carboxylic acid derivative (**32**, *Pf*NF54 $IC_{50}$ > 6 μM). Furthermore, ethyl ester **33** bearing a 4-CN-benzyl group retains comparable potency in the MDR strain *Pf*K1 (RI = 1.21) compared to the 4-F-benzyl match pair **34**, in which the resistance index is higher (RI = 2.83). The low solubility and susceptibility of the ester structural motif to metabolism (Table 3) pre-empted the further exploration of bioisosteres.

Amides are utilized as ester group bioisosteres; additionally, amidation is a known strategy for reducing hERG affinity and improving aqueous solubility. [16,17] Therefore, we accordingly prepared and evaluated amides at the 4-position in the lateral phenyl group while maintaining either a 4-F or 4-CN group in the benzyl portion (Table 3). However, these AST amide analogues **43**–**53** produced lower activities (*Pf*NF54 $IC_{50}$ = 0.199–1.91 μM) compared to those of the ester match pairs (**33** and **34**) and AST, although the desired increase in solubility was achieved in some of the amides, especially those that contained water-solubilizing groups (**43**–**46**).

**Table 3.** In Vitro Antiplasmodium and solubility of AST Analogues in SAR 2 (ND, Not Determined)

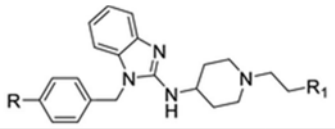

| Compound | R | $R_1$ | $R_2$ | *Pf* $IC_{50}$ (μM)[a,b] NF54 | *Pf* $IC_{50}$ (μM)[a,b] K1 | RI[c] | Sol.[d] (μM) |
|---|---|---|---|---|---|---|---|
| **27** | CN | 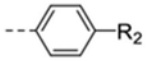 | H | 0.163 | 0.170 | 1.04 | 40 |
| **28** | | | $SO_2Me$ | 0.238 | 4.592 | - | 80 |
| **29** | | | $CH_3$ | 0.357 | ND | - | 40 |
| **30** | | | $CF_3$ | 0.035 | 0.103 | 2.94 | 20 |
| **31** | | | $CO_2Me$ | 0.204 | ND | - | 80 |
| **32** | | | $CO_2H$ | >6 | ND | - | 120 |
| **33** | | | $CO_2Et$ | 0.043 | 0.052 | 1.21 | 40 |
| **34** | F | | $CO_2Et$ | 0.067 | 0.19 | 2.83 | 65 |
| **35** | CN |  | - | 4.152 | ND | - | 20 |
| **36** | |  | - | 1.386 | ND | - | 20 |
| **37** | |  | - | 1.248 | ND | - | <5 |
| **38** | | 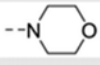 | - | >6 | ND | - | 10 |
| **39** | | 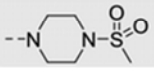 | - | >6 | ND | - | 40 |
| **40** | |  | - | 1.542 | ND | - | <10 |
| **41** | |  | - | 1.677 | ND | - | 20 |
| **43** | F | 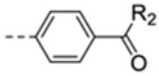 | 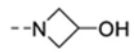 | 0.640 | ND | - | 150 |
| **44** | | | 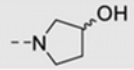 | 1.810 | ND | - | 200 |
| **45** | | |  | 1.613 | ND | - | 72 |
| **46** | | | 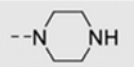 | 0.199 | 1.136 | 5.71 | 200 |
| **47** | CN | 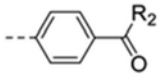 |  | 0.318 | ND | - | 30 |
| **48** | | |  | 1.912 | ND | - | ND |
| **49** | | |  | 0.295 | ND | - | <5 |
| **50** | | | 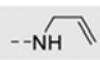 | 0.314 | ND | - | ND |
| **51** | | | 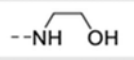 | 0.759 | ND | - | 50 |
| **52** | | | 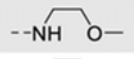 | 0.755 | ND | - | 100 |
| **53** | | | 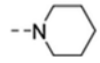 | 0.249 | ND | - | 5 |

[a]Mean from $n \geq 2$ independent experiments with sensitive (NF54) and multi-drug-resistant (K1) strains of *Pf*. [b]Chloroquine (NF54 $IC_{50}$ = 0.004 μM; K1 $IC_{50}$ = 0.14 μM) was used as a reference drug for activity. [c]Resistance index = [*Pf*K1 $IC_{50}$/*Pf*NF54 $IC_{50}$]. [d]Solubility, determined using turbidimetric method at pH 7.4. Hydrocortisone (>200 μM) and reserpine (<10 μM) were used as control drugs.

Notably, secondary amides (**47**, **49**–**52**) generally displayed activity higher than that of tertiary amides (**43**–**45** and **48**), although as a caveat, some of these tertiary amides (**43**–**45**) contain other structural features that may contribute to low activity. The 3-hydroxyazetidine amide (**43**, *Pf*NF54 $IC_{50}$ = 0.640 μM) displayed activity more than 2-fold higher than that of the pyrrolidine (**44**, *Pf*NF54 $IC_{50}$ = 1.81 μM) and piperidine (**45**, *Pf* NF54 $IC_{50}$ = 1.61 μM) analogues, both of which had comparable activities. The phenyl moiety was found to be crucial for potency (**27**, *Pf*NF54 $IC_{50}$ = 0.163 μM) as its replacement with either aromatic or aliphatic heterocycles led to a significant loss in potency (**35**–**41**, *Pf*NF54 $IC_{50}$ > 1.2 μM, Table 3) compared to that of both **27** and AST. Following the assessment of representative compounds from each compound class, 4-$CF_3$**30**, 4-$CO_2$Et **34**, and methyl amide **47** displayed high β-H inhibition, with $IC_{50}$ values of <100 μM (Table S1). Most analogues in this SAR exhibited low to moderate solubility (Sol = 10–100 μM), with some amides showing high solubility.

To assess potential for transmission blocking, a selected number of compounds across the four SARs were evaluated against early gametocyte (EG, stages I–III) and late gametocyte (LG, stage IV/V) stages in a dual-point screen at 1.0 and 5.0 μM (Table S2 in the Supporting Information). Compounds **2**, **7**, and **8** displayed high activity (>70% at 5 μM, or >50% at 1 μM), with $IC_{50}$ values in the low micromolar range and stage specificity toward EGs, defined as compounds that show a ≥2-fold change in dual-point values between EG and LG. However, these compounds generally exhibited loss of activity following $IC_{50}$ determination, a phenomenon that is not surprising and may be attributable to confounding factors in the assay such as freeze–thawing cycles. Comparatively, AST, **4**, and **46** showed activity and stage specificity toward LG, with $IC_{50}$ values lower than that of active compounds on EG. Of these active compounds against the LG, piperazine amide **46** exhibited the highest potency (*Pf*LG $IC_{50}$ = 0.6 ± 0.1 μM, Table S2), indicating it as a potential transmission-blocking candidate.

Representative compounds and those with antiplasmodium activity of *Pf*NF54 $IC_{50}$ < 0.2 μM were assessed for cytotoxicity in the Chinese hamster ovary (CHO) cell line. Accordingly, structurally diverse analogues with favorable antiplasmodium activity were evaluated for their hERG inhibition using potassium channels expressed in the CHO cell line on an automated Q-patch clamp platform (Table 4). Additionally, microsomal metabolic stability of compounds displaying low cytotoxicity (SI > 100) were evaluated in human, rat, and mouse liver microsomes (HLMs, RLMs, and MLMs, respectively, Table S3, Supporting Information).

**Table 4.** In Vitro Cytotoxicity (CHO), hERG Channel Activity, and Microsomal Metabolic Stability Data of Selected Analogues

| | cytotoxicity (CHO)[a] | | hERG[b] | | |
|---|---|---|---|---|---|
| **compound** | **$IC_{50}$ (μM)** | **SIc** | **$IC_{50}$ (μM)** | **SIc** | **clog*P*d** |
| AST | 29.6 | 344 | 0.0042 | 0.049 | 5.70 |
| **3** | | | 0.41 | 1.24 | 4.65 |
| **12** | | | 0.09 | 0.16 | 3.80 |
| **14** | | | 0.05 | 0.32 | 4.70 |
| **16** | | | 0.11 | 0.23 | 4.07 |
| **18** | | | 4.16 | >0.7 | 4.45 |
| **21** | >50 | >2000 | 0.97 | 38.8 | 4.83 |
| **24** | 47.4 | 667 | 0.05 | 0.70 | 4.85 |
| **30** | 5.36 | 153 | | | 5.71 |
| **32** | 12.4 | 289 | | | 5.22 |
| **34** | 42.3 | 631 | | | 5.69 |
| **46** | 29.5 | 148 | 8.61 | 43.3 | 3.49 |
| verapamil | | | 0.2–0.8 | | |
| emetine | 0.95 | | | | |

[a]CHO: Chinese hamster ovary epithelial cell line. Mean value from $n = 3$ independent experiments. Emetine ($IC_{50}$ = 0.033 μM) was used as the reference drug. [b]hERG: Human ether-a-go-go-related gene. Mean value from $n = 3$ independent experiments. Verapamil ($IC_{50}$ = 0.56 ± 0.096 μM) as a reference. [c]SI: Selectivity index = [CHO $IC_{50}$/*Pf*NF54 $IC_{50}$] or [hERG $IC_{50}$/*Pf*NF54 $IC_{50}$]. [d]Calculated using StarDrop software v6.5-1-1.

All tested compounds showed high selectivity (SI > 148) against CHO cells (Table 4). Compounds **21** (hERG $IC_{50}$ = 0.97 μM) and **46** (hERG $IC_{50}$ = 8.61 μM) displayed the lowest hERG channel inhibition activity with 202-fold and 1790-fold higher $IC_{50}$ values compared to those of AST (hERG $IC_{50}$ = 0.0042 μM). However, the low hERG selectivity (SI < 43.3) of compounds remains a challenge that needs to be further addressed. Notably, carboxylic acid analogue **18** (hERG $IC_{50}$ = 4.16 μM) also displayed low hERG activity potentially attributable to its zwitterionic furnishing properties; however, the presence of a carboxylic acid group is often associated with poor absorption and limited membrane permeability and may thus explain the equally observed weak whole-cell antiplasmodium activity (*Pf*NF54 $IC_{50}$ > 6 μM).

Microsomal metabolic stability was generally low, especially in rodent species (M/RLM < 45% remaining and $CL_{int}$ > 67 $\mu L \cdot min^{-1} \cdot mg^{-1}$, Table S2) compared to that of human-derived microsomes. Therefore, none of the compounds could be progressed for in vivo antimalarial evaluation in mice.

In conclusion, 46 analogues were synthesized and evaluated for their antiplasmodium activity and solubility. Overall, we highlight modifications that lead to improved antiplasmodium activity, solubility, and hERG channel inhibition activity. Cytotoxicity of tested compounds was low, although metabolic stability and marginal selectivity for antiplasmodium activity over hERG affinity still remains a challenge in the development of AST analogues as antimalarial agents. SAR explorations have demonstrated the significance of the 4-aminopiperidine linker and the phenethyl moiety and the importance of adequate basicity of the piperidine nitrogen. We further showed that F/CN disubstitution is tolerated in the benzyl moiety and that replacement of either 4-F or 4-OMe groups in AST with nitrile broadly produces equipotent analogues. Additionally, replacement of 4-F or 4-OMe groups in AST with EWGs such as $CF_3$ significantly improves the potency. From this study, incorporation of 4-$CF_3$-3-pyridyl moiety on the benzyl portion while retaining the 4-CN in the lateral phenyl group produced the most potent analogue (**21**, *Pf*NF54 $IC_{50}$ = 0.025 μM) with low hERG channel activity (hERG $IC_{50}$ = 0.97, SI = 38.8).

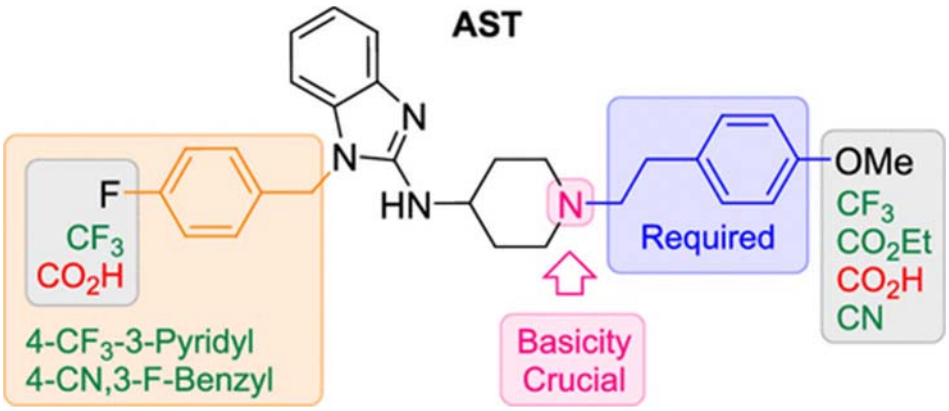


**Figure 2.** Summary of SAR trend around AST derived from this series.

Exploration of potential substituents at the 4-phenyl position of debenzylated analogue (**12**) is warranted, as these are envisaged to produce low molecular weight analogues with improved physicochemical and solubility profiles. Additionally, the potential for blood-stage/LG dual activity and the low hERG affinity of **46** presents an opportunity for further optimization. Furthermore, ester analogue **33** is amenable for exploration of other ester bioisosteric replacements to mitigate the underlying metabolic liability associated with the ester group.

## Acknowledgement

Support was provided by University of Cape Town, South African Medical Research Council (K.C.) and the South African Research Chairs Initiative of the Department of Science and Technology administered through the South African National Research Foundation are acknowledged for their support (K.C. UID: 64767 and L.B. UID: 84627) and a NRF Community of Practice on “Evaluating Malaria Control Interventions” (L.B. and K.C.; UID: 110666).

## Abbreviations

| | |
|---|---|
| AST | astemizole |
| DMAST | desmethylastemizole |
| hERG | human ether-a-go-go-related gene |
| SI | selectivity index |
| CQ | chloroquine |
| AQ | amodiaquine |
| CHO | Chinese hamster ovary |
| HTS | high-throughput screening |
| SAR | structure–activity relationship |
| $I_{Kr}$ | potassium ion current |
| ND | not determined |
| $IC_{50}$ | concentration of a drug that is required for 50% inhibition in vitro |

## References


**1** Cox, F. E. History of Human Parasitic Diseases. *Infect. Dis. Clin. North Am.* **2004**, *18* (2), 171– 188, DOI: 10.1016/j.idc.2004.01.001

**2** Yoeli, M. Sir Ronald Ross and the Evolution of Malaria Research. *Bull. N. Y. Acad. Med.* **1973**, *49* (8), 722– 735

**3** World Health Organization. *World Malaria Report 2020*, Geneva, 2020.

**4** Tse, E. G.; Korsik, M.; Todd, M. H. The Past, Present and Future of Anti-Malarial Medicines. *Malar. J.* **2019**, *18* (1), 93, DOI: 10.1186/s12936-019-2724-z

**5** White, N. J.; Nosten, F. Artemisinin-Based Combination Treatment of Falciparum Malaria. *Am. J. Trop. Med. Hyg.* **2007**, *77*, 181– 192, DOI: 10.4269/ajtmh.2007.77.181

**6** Noedl, H.; Se, Y.; Schaecher, K.; Smith, B. L.; Socheat, D.; Fukuda, M. M. Evidence of Artemisinin-Resistant Malaria in Western Cambodia. *N. Engl. J. Med.* **2008**, *359* (24), 2619–2620, DOI: 10.1056/NEJMc0805011

**7** Uwimana, A.; Umulisa, N.; Venkatesan, M.; Svigel, S. S.; Zhou, Z.; Munyaneza, T.; Habimana, R. M.; Rucogoza, A.; Moriarty, L. F.; Sandford, R.; Piercefield, E.; Goldman, I.; Ezema, B.; Talundzic, E.; Pacheco, M. A.; Escalante, A. A.; Ngamije, D.; Mangala, J. N.; Kabera, M.; Munguti, K.; Murindahabi, M.; Brieger, W.; Musanabaganwa, C.; Mutesa, L.; Udhayakumar, V.; Mbituyumuremyi, A.; Halsey, E. S.; Lucchi, N. W. Association of Plasmodium Falciparum Kelch13 R561H Genotypes with Delayed Parasite Clearance in

Rwanda: An Open-Label, Single-Arm, Multicentre, Therapeutic Efficacy Study. *Lancet Infect. Dis.* **2021**, DOI: 10.1016/S1473-3099(21)00142-0

**8** Chong, C. R.; Chen, X.; Shi, L.; Liu, J. O.; Sullivan, D. J. A Clinical Drug Library Screen Identifies Astemizole as an Antimalarial Agent. *Nat. Chem. Biol.* **2006**, *2*, 415– 416, DOI: 10.1038/nchembio806

**9** Derbyshire, E. R.; Prudêncio, M.; Mota, M. M.; Clardy, J. Liver-Stage Malaria Parasites Vulnerable to Diverse Chemical Scaffolds. *Proc. Natl. Acad. Sci. U. S. A.* **2012**, *109* (22), 8511– 8516, DOI: 10.1073/pnas.1118370109

**10** Musonda, C. C.; Whitlock, G. A.; Witty, M. J.; Brun, R.; Kaiser, M. Chloroquine-Astemizole Hybrids with Potent in Vitro and in Vivo Antiplasmodial Activity. *Bioorg. Med. Chem. Lett.* **2009**, *19*, 481– 484, DOI: 10.1016/j.bmcl.2008.11.047

**11** Roman, G.; Crandall, I. E.; Szarek, W. A. Synthesis and Anti- Plasmodium Activity of Benzimidazole Analogues Structurally Related to Astemizole. *ChemMedChem* **2013**, *8*, 1795– 1804, DOI: 10.1002/cmdc.201300172

**12** Tian, J.; Vandermosten, L.; Peigneur, S.; Moreels, L.; Rozenski, J.; Tytgat, J.; Herdewijn, P.; Van den Steen, P. E.; De Jonghe, S. Astemizole Analogues with Reduced HERG Inhibition as Potent Antimalarial Compounds. *Bioorg. Med. Chem.* **2017**, *25* (24), 6332– 6344, DOI: 10.1016/j.bmc.2017.10.004

**13** Kumar, M.; Okombo, J.; Mambwe, D.; Taylor, D.; Lawrence, N.; Reader, J.; van der Watt, M.; Fontinha, D.; Sanches-Vaz, M.; Bezuidenhout, B. C.; Lauterbach, S. B.; Liebenberg, D.; Birkholtz, L.; Coetzer, T. L.; Prudêncio, M.; Egan, T. J.; Wittlin, S.; Chibale, K. Multistage Antiplasmodium Activity of Astemizole Analogues and Inhibition of Hemozoin Formation as a Contributor to Their Mode of Action. *ACS Infect. Dis.* **2019**, *5* (2), 303– 315, DOI: 10.1021/acsinfecdis.8b00272

**14** Fleming, F. F.; Yao, L.; Ravikumar, P. C.; Funk, L.; Shook, B. C. Nitrile-Containing Pharmaceuticals: Efficacious Roles of the Nitrile Pharmacophore. *J. Med. Chem.* **2010**, *53* (22), 7902– 7917, DOI: 10.1021/jm100762r

**15** Tong, A. S. T.; Choi, P. J.; Blaser, A.; Sutherland, H. S.; Tsang, S. K. Y.; Guillemont, J.; Motte, M.; Cooper, C. B.; Andries, K.; Van den Broeck, W.; Franzblau, S. G.; Upton, A. M.; Denny, W. A.; Palmer, B. D.; Conole, D. 6-Cyano Analogues of Bedaquiline as Less Lipophilic and Potentially Safer Diarylquinolines for Tuberculosis. *ACS Med. Chem. Lett.* **2017**, *8* (10), 1019– 1024, DOI: 10.1021/acsmedchemlett.7b00196

**16** Skerlj, R.; Bridger, G.; Zhou, Y.; Bourque, E.; McEachern, E.; Danthi, S.; Langille, J.; Harwig, C.; Veale, D.; Carpenter, B.; Ba, T.; Bey, M.; Baird, I.; Wilson, T.; Metz, M.; MacFarland, R.; Mosi, R.; Bodart, V.; Wong, R.; Fricker, S.; Huskens, D.; Schols, D. Mitigating HERG Inhibition: Design of Orally Bioavailable CCR5 Antagonists as Potent Inhibitors of R5 HIV-1 Replication. *ACS Med. Chem. Lett.* **2012**, *3*, 216– 221, DOI: 10.1021/ml2002604

**17** Nair, A. G.; Wong, M. K. C.; Shu, Y.; Jiang, Y.; Jenh, C.-H.; Kim, S. H.; Yang, D.-Y.; Zeng, Q.; Shao, Y.; Zawacki, L. G.; Duo, J.; McGuinness, B. F.; Carroll, C. D.; Hobbs, D.

W.; Shih, N.; Rosenblum, S. B.; Kozlowski, J. A. IV. Discovery of CXCR3 Antagonists Substituted with Heterocycles as Amide Surrogates: Improved PK, HERG and Metabolic Profiles. *Bioorg. Med. Chem. Lett.* **2014**, *24* (4), 1085– 1088, DOI: 10.1016/j.bmcl.2014.01.009